ACS SyntheticBiology

Research Article

pubs.acs.org/synthbio

Programming Controlled Adhesion of *E. coli* to Target Surfaces, Cells, and Tumors with Synthetic Adhesins

Carlos Piñero-Lambea,[†,§] Gustavo Bodelón,[†,§] Rodrigo Fernández-Periáñez,[‡] Angel M. Cuesta,[‡] Luis Álvarez-Vallina,[‡] and Luis Ángel Fernández*[,†]

[†]Department of Microbial Biotechnology, Centro Nacional de Biotecnología (CNB), Consejo Superior de Investigaciones Científicas (CSIC), Campus UAM Cantoblanco, 28049 Madrid, Spain

[‡]Molecular Immunology Unit, Hospital Universitario Puerta de Hierro, Majadahonda, 28222 Madrid, Spain

Supporting Information

ABSTRACT: In this work we report synthetic adhesins (SAs) enabling the rational design of the adhesion properties of *E. coli*. SAs have a modular structure comprising a stable β-domain for outer membrane anchoring and surface-exposed immunoglobulin domains with high affinity and specificity that can be selected from large repertoires. SAs are constitutively and stably expressed in an *E. coli* strain lacking a conserved set of natural adhesins, directing a robust, fast, and specific adhesion of bacteria to target antigenic surfaces and cells. We demonstrate the functionality of SAs *in vivo*, showing that, compared to wild type *E. coli*, lower doses of engineered *E. coli* are sufficient to colonize solid tumors expressing an antigen recognized by the SA. In addition, lower levels of engineered bacteria were found in non-target tissues. Therefore, SAs provide stable and specific adhesion capabilities to *E. coli* against target surfaces of interest for diverse applications using live bacteria.

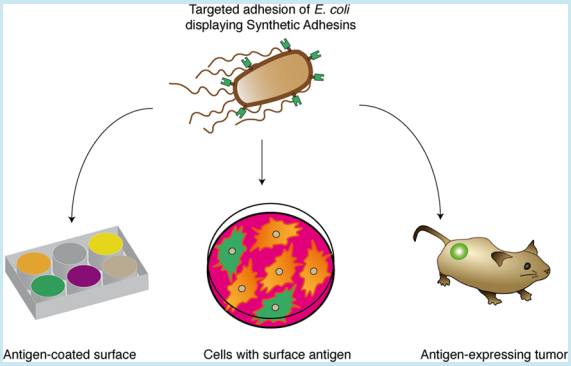

KEYWORDS: *adhesins, cell surface antigens, E. coli, synthetic biology, tumor targeting*

One of the aims of synthetic biology is the rational design of microorganisms for biotechnological applications.[1] An important aspect for the design of these tailored microorganisms is the molecular composition of their cell surface, which determines their interaction with the environment. Incorporation of affinity ligands on the surface of the engineered cell could help to program its adhesion properties toward a target surface or cell of interest. Natural bacteria encode in their genomes diverse types of adhesive proteins, termed adhesins, which play a fundamental role in multiple processes (e.g., biofilm formation, host-colonization, cell invasion) by recognizing molecular structures found in abiotic and biotic surfaces of other bacteria, plant, and animal cells.[2,3] However, the variety and redundancy of natural adhesins, together with the widespread distribution of their receptors among different cell types and surfaces, preclude their use as functional units conferring predictable adhesion capabilities.

E. coli is a common host for biotechnological applications due to its amenability for genetic manipulation and heterologous protein expression.[4,5] Although some *E. coli* isolates have acquired pathogenicity traits, most strains of this Gram-negative bacterium are nonpathogenic commensals of the gastrointestinal (GI) tract of vertebrates.[6] Interestingly, *E. coli* has shown potential for *in vivo* biomedical applications against infections agents and cancer. Specific *E. coli* strains have been used in humans as probiotics competing with pathogenic bacteria causing infections in the mucosal surfaces of the GI and urinary tracts.[7,8] In addition, commensal and probiotic *E. coli* strains administered systemically have been shown to colonize solid tumors grafted subcutaneously in mice.[9,10] Hence, engineering the adhesion properties of these nonpathogenic *E. coli* strains may improve their colonization efficiency and specificity for target mucosal surfaces and tumors *in vivo*.

In this work we report synthetic adhesins (SAs) that allow the rational design of robust and specific adhesion capacities to *E. coli*. SAs have a modular structural organization resembling that of natural *E. coli* adhesins, which are commonly composed of an anchor β-barrel module that is embedded in the bacterial outer membrane (OM) and an adhesion module bearing an immunoglobulin (Ig)-like fold that is exposed to the extracellular milieu.[2,11] The designed SAs combine a highly stable β-barrel domain derived from intimin, an adhesin found in enterohemorrhagic and enteropathogenic *E. coli* strains (EHEC and EPEC, respectively),[12,13] with Ig domains of high affinity, solubility, and stability based on the variable domain of heavy chain-only antibodies (HCAbs), known as VHHs (VH of HCAbs) or nanobodies.[14] VHHs of defined specificity can be selected against antigens of interest from large VHH repertories cloned and expressed in *E. coli* and its bacteriophages.[14,15]

Received: May 20, 2014
Published: July 21, 2014

We show that SAs integrated in the chromosome of *E. coli* can be constitutively expressed, being nontoxic and stably maintained throughout multiple bacterial generations *in vitro* and *in vivo* in the absence of inducer and selection pressure. Expression of SAs in an engineered *E. coli* chassis devoid of a set of natural adhesins directed the specific adhesion of bacteria to abiotic surfaces and mammalian cells expressing on their surface the target molecule recognized by the SA. Importantly, *in vivo* experiments showed that low doses of the engineered bacteria colonize solid tumors expressing the target molecule with higher efficiency than the wild type *E. coli* strain, having also lower retention in normal organs.

RESULTS AND DISCUSSION

Structure of Synthetic Adhesins and Targeted Adhesion of *E. coli* to Antigenic Surfaces. Although Ig-fragments have been displayed on the surface of *E. coli* with various expression systems,[11] such as lipoprotein fusions[16] and β-domains of autotransporters,[17] adhesion of *E. coli* to target surfaces has not been observed with those systems. Lipoprotein fusions severely disturb the integrity of the OM causing significant leakiness and toxicity,[18] whereas autotransporters are prone to proteolysis as part of their secretion mechanism.[19] Recently, we reported that libraries of VHH can be displayed on the surface of *E. coli* cells fused to an N-terminal fragment of intimin from EHEC (residues 1−659; named Neae), allowing the isolation of high affinity clones binding an antigen of interest.[15] The Neae polypeptide (ca. 69 kDa) comprises the native intimin signal peptide (SP), LysM domain for peptidoglycan binding, a 12-stranded β-barrel domain for OM insertion, and a surface-exposed Ig-like domain (named D0) lacking adhesion capacity (Figure 1a).[12,13] VHH domains (ca. 13 kDa) are fused to the C-end of Neae generating protein fusions termed NVHH with a total mass of ca. 84 kDa and tagged with E- and myc-tag epitopes (Figure 1a).

To investigate whether NVHH fusions could modify the adhesion properties of *E. coli*, we first examined the specific adhesion of bacteria to abiotic surfaces coated with the antigen recognized by the VHH. To this end, NVHH fusions binding GFP (NVgfp) and human fibrinogen (NVfib) were expressed in *E. coli* K-12 strain EcM1 (MG1655Δ*fim*A-H; Supplementary Table 1). This strain has a deletion of the *fimA-H* operon encoding type 1 fimbriae, a natural adhesin found in most *E. coli* strains and involved in recognition of mannosylated glycoproteins found on epithelial cell surfaces.[20] Cultures of EcM1 bacteria bearing plasmids encoding NVgfp, NVfib, and Neae (Supplementary Table 1), were induced with IPTG, and the display of the NVHH protein fusions on the surface of *E. coli* was confirmed by flow cytometry with anti-myc monoclonal antibody (mAb) (Figure 1b). Induced bacteria were incubated on GFP- and fibrinogen (Fib)-coated plastic surfaces, washed with PBS, and stained with crystal violet to reveal the presence of bound bacteria. This experiment demonstrated the specific binding to those surfaces coated with the antigen recognized by the corresponding NVHH fusion (Figure 1c). Specific adhesion of *E. coli* bacteria was confirmed by light microscopy (Figure 1d). These results indicated that NVHH fusions could act as SAs driving the adhesion of *E. coli* bacteria to a target surface.

Constitutive, Stable, and Nontoxic Expression of SAs from the Chromosome of *E. coli*. To further investigate *E. coli* targeting mediated by SAs, we developed constitutive gene expression cassettes that can be integrated as a single copy in

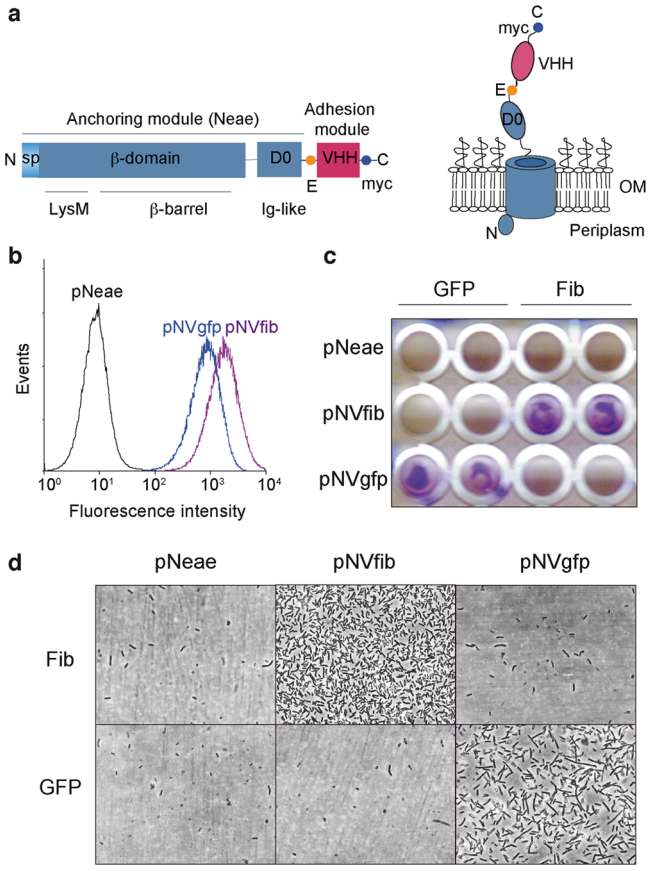

Figure 1. Synthetic adhesins and targeting of *E. coli* cells to antigens immobilized on a plastic surface. (a) Scheme of the primary structure of SAs (left) showing the N-terminal domain of intimin (Neae) as anchoring module, comprising the signal peptide (SP), LysM, β-barrel, and D0 Ig-like domains, fused to a variable Ig domain from heavy-chain-only antibodies (VHH) as adhesion module. The E-tag and myc-tag epitopes flanking the VHH domain are also indicated. Model of a SA fusion protein (right) in the bacterial outer membrane (OM) with the VHH exposed to the extracellular milieu. (b) Flow cytometry analysis of IPTG-induced *E. coli* EcM1 bearing pNeae (control), pNVgfp, or pNVfib plasmids. Histograms show the fluorescence intensity of bacteria stained with anti-myc mAb and secondary anti-mouse IgG-Alexa 488. (c) Induced *E. coli* EcM1 expressing the Neae polypeptide control (pNeae) or SAs against GFP (pNVgfp) or human fibrinogen (pNVfib) were incubated with plastic surfaces coated with GFP or human fibrinogen (Fib), as indicated. Bacterial adhesion was assessed by crystal violet staining. (d) Adhesion of *E. coli* bacteria to target antigen-coated plastic surface (as in panel c) observed under the light microscope.

the chromosome of *E. coli*. This strategy would allow constant expression of the SA in the absence of exogenous inducers and antibiotics for plasmid maintenance. For site-specific integration in the chromosome of *E. coli*, we adapted a marker-less gene deletion strategy that enables sequential manipulation of multiple gene loci leaving no antibiotic resistance genes or any other vector sequences in the chromosome.[21] This technology is based on the insertion of a suicide plasmid bearing homology regions (HRs) of the targeted gene and the subsequent generation of double-strand breaks by expression of I-SceI restriction endonuclease *in vivo*, which are repaired, resulting in the specific modification of the targeted gene (Supplementary Figure S1). For this we constructed a suicide vector with I-SceI sites, named pGE (Supplementary Table 1), and generated

dx.doi.org/10.1021/sb500252a | *ACS Synth. Biol.* 2015, 4, 463−473

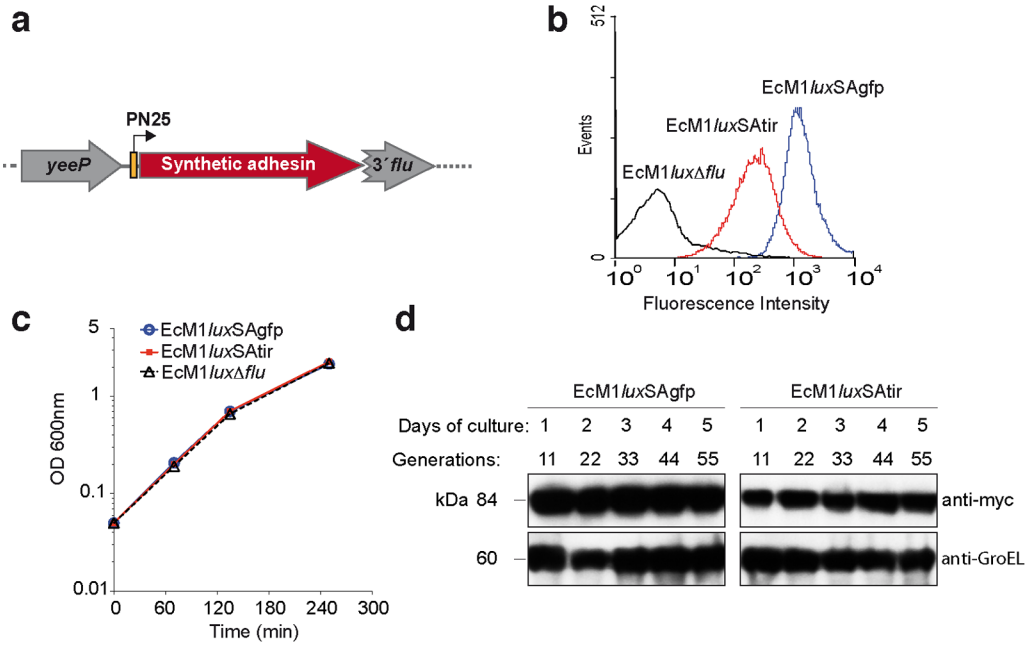

Figure 2. Constitutive, stable, and nontoxic expression of synthetic adhesins from the chromosome of *E. coli*. (a) Scheme of a SA gene fusion integrated in the *flu* gene of *E. coli* chromosome under the control of the constitutive promoter P_{N25}. (b) Flow cytometry analysis of *E. coli* EcM1*lux*Δ*flu*, EcM1*lux*SAgfp, or EcM1*lux*SAtir bacteria. Histograms show the fluorescence intensity of bacteria stained with anti-myc mAb and secondary anti-mouse IgG-Alexa 488. (c) Growth curves of bacterial cultures of the same strains shown in panel b. (d) Western blot analysis of the expression of SAs in EcM1*lux*SAgfp and EcM1*lux*SAtir strains grown in LB cultures for the indicated time. SAs were immunodetected with anti-myc tag mAb. Cytoplasmic GroEL chaperone was used as loading control (lower panel) and was detected with anti-GroEL mAb.

derivatives for integration of SAs having VHHs binding GFP (pGE*flu*-SAgfp) or binding TirM (pGE*flu*-SAtir).[15] TirM is the extracellular domain (residues 252−360) of the translocated intimin receptor of EHEC.[22] These constructs incorporated a constitutive promoter, P_{N25},[23] driving the expression of the SA, and HRs flanking the *flu* gene of *E. coli* K-12 strain MG1655. The *flu* gene encodes Antigen 43, an adhesin conserved in most *E. coli* strains that is involved in biofilm formation and bacterial self-aggregation.[24] Using these vectors the *flu* gene of *E. coli* EcM1 was replaced by the gene cassettes expressing SAgfp or SAtir (Figure 2a), generating strains EcM1SAgfp and EcM1SAtir (Supplementary Table 1). We also generated with suicide plasmid pGE*flu* the control strain EcM1Δ*flu*, an isogenic EcM1 strain not expressing SAs and having a deletion of *flu* identical to that generated by the insertion of SAs. Finally, these strains were tagged with a bioluminescent reporter, the *luxCDABE* operon from *Photorhabdus luminescens*[25] under the control of a constitutive promoter (P_2), which was inserted in the *matBCDEF* operon with suicide vector pGE*mat-lux* (Supplementary Table 1). This operon encodes the meningitis-associated and temperature-regulated Mat fimbriae, also termed *E. coli* common pilus, which are produced by most *E. coli* pathogroups, being involved in early stage biofilm development and host cell recognition.[26] The final bioluminescent strains were named EcM1*lux*Δ*flu*, EcM1*lux*SAgfp, and EcM1*lux*SAtir (Supplementary Table 1).

Flow cytometry analysis of EcM1*lux*SAgfp and EcM1*lux*SAtir with anti-myc mAb (Figure 2b) indicated that both SAs were highly and homogeneously expressed on the surface of bacteria, SAgfp being expressed at higher levels than SAtir. EcM1*lux*SAgfp and EcM1*lux*SAtir strains showed identical growth curves as EcM1*lux*Δ*flu* in LB media at 37 °C with agitation (Figure 2c), and nearly identical colony forming units (CFU) per unit of optical density at 600 nm (OD_{600}) were determined by plating (~1.0×10^9 CFU/OD_{600}), demonstrating that bacterial growth and viability was not affected by the constitutive expression of the SAs. In addition, EcM1*lux*SAgfp and EcM1*lux*SAtir strains were grown at 37 °C for 5 days with a daily dilution (1:2000) in fresh LB medium lacking antibiotics. Whole-cell protein extracts were prepared from each culture harvested every day and analyzed by Western blot with anti-myc mAb (to detect the SA) and anti-GroEL mAb, as loading control, demonstrating that the expression of the SAs was stably maintained throughout the length of the experiment (ca. 55 bacterial generations) without the need of any inducer or antibiotic pressure (Figure 2d). Similarly, the *lux* operon was stably expressed in both strains along the experiment (Supplementary Figure S2).

Adhesion of Engineered *E. coli* to Antigens Expressed on the Surface of Mammalian Cells. We investigated whether EcM1*lux*SAgfp and EcM1*lux*SAtir bacteria adhered specifically to *in vitro* cultured mammalian cells expressing on their surface the cognate antigens recognized by the SAs. As an experimental model, we stably transfected HeLa cells with plasmids pDisplay-GFP-tm and pDisplay-TirM-tm (Supplementary Table 1), which expressed GFP and TirM antigens, respectively, on the extracellular side of the plasma membrane by means of an N-terminal signal peptide and a C-terminal transmembrane (tm) anchor domain from the platelet derived growth factor receptor (PDGFR) (Supplementary Figure S3a). In addition, the protein fusion containing TirM incorporates, before the tm domain, the monomeric green fluorescent protein mWasabi.[27,28] The primary sequence of mWasabi differs from that of GFP and is not recognized by the VHH cloned in SAgfp.[28,29] Thus, expression of GFP-tm and TirM-tm fusion proteins on the surface of HeLa cells can be monitored by their green fluorescence emission. Upon stable transfection, fluorescence-positive HeLa cells were enriched by fluorescence-

dx.doi.org/10.1021/sb500252a | *ACS Synth. Biol.* 2015, 4, 463−473

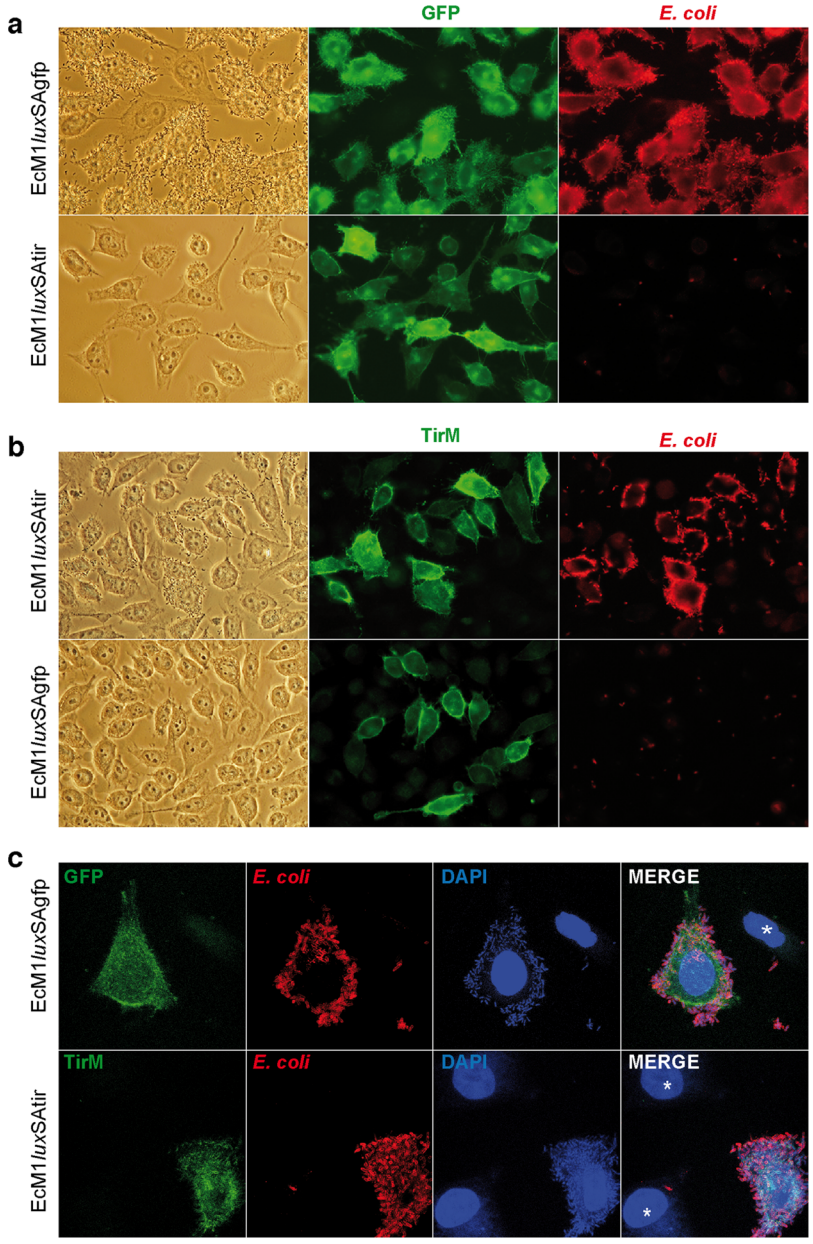

Figure 3. Adhesion of *E. coli* expressing synthetic adhesins to target mammalian cells. (a) Light and fluorescence microscopy images of HeLa-GFP-tm cells grown in culture and infected with EcM1*lux*SAgfp or EcM1*lux*SAtir bacteria (MOI 300:1), as indicated. Expression of GFP-tm fusion on the surface of these cells is detected by the green fluorescence emission. (b) Light and fluorescence microscopy images of HeLa-TirM-tm cells grown in culture and infected with EcM1*lux*SAgfp or EcM1*lux*SAtir bacteria (MOI 300:1), as indicated. Expression of TirM-tm fusion on the surface of these cells is detected by the green fluorescence emission of its mWasabi domain. Bacteria were stained with anti-*E. coli* polyclonal serum and anti-IgG-rabbit-Alexa-594 (red). (c) Confocal microscopy images of HeLa-GFP-tm cells infected with EcM1*lux*SAgfp (top panels) and HeLa-TirM-tm cells infected with EcM1*lux*SAtir (bottom panels). Infection and staining was carried out as in panels a and b. In addition, cell nuclei and bacterial chromosomes were stained with DAPI (blue). The selected images contain antigen-negative cells (labeled with asterisks) to show the absence of bound bacteria to them.

activated cell sorting (FACS) and expanded *in vitro*. The expanded cell populations, named HeLa-GFP-tm and HeLa-TirM-tm, contained cells with different expression levels of these antigens on their surface, including some cells with undetectable levels of the antigens, especially in HeLa-TirM-tm (Supplementary Figure S3b).

We performed *in vitro* adhesion assays of HeLa-GFP-tm and HeLa-TirM-tm cultures infected with EcM1*lux*SAgfp or EcM1*lux*SAtir bacteria (MOI 300:1). After 1 h infection, unbound bacteria were removed with PBS, and the samples were stained with anti-*E. coli* polyclonal antibodies and DAPI (to stain DNA). Inspection of the samples by light and fluorescence microscopy (Figure 3) revealed very high numbers of EcM1*lux*SAgfp and EcM1*lux*SAtir bacteria (red fluorescence) specifically adhered to HeLa cells expressing GFP or TirM, respectively (green fluorescence). Target HeLa cells were largely covered by bound bacteria expressing the corresponding SA, as can be also visualized by three-dimensional reconstruction of confocal images (Supplementary Video 1). In contrast, EcM1*lux*SAgfp and EcM1*lux*SAtir bacteria were not bound to HeLa cells expressing the nonspecific antigen (i.e., TirM for EcM1*lux*SAgfp; GFP for EcM1*lux*SAtir) (Figure 3a and b).

dx.doi.org/10.1021/sb500252a | *ACS Synth. Biol.* 2015, 4, 463−473

Importantly, bacteria adhered to cells with different expression levels of the target antigen on their surface, but not to antigen-negative cells that can be found in both HeLa-GFP-tm and HeLa-TirM-tm cultures (labeled with asterisks in Figure 3c). Similar results were observed with lower MOI and infection times (see below). We also tested whether the bioluminescent reporter could provide a sensitive readout of the bacterial adhesion process. To this end, HeLa, HeLa-GFP-tm, and HeLa-TirM-tm cells were grown in a multiwell tissue culture plate and infected as above with EcM1*lux*SAgfp, EcM1*lux*SAtir, or EcM1*lux*Δ*flu*. After 1 h infection, the plate was washed with PBS and monitored for light emission. Bioluminescence signals were observed only in those wells in which bacteria expressing SAs infected HeLa cells expressing the cognate target antigen (Supplementary Figure S4).

To gain further insight into the adhesion process mediated by the SAs, we performed time-lapse live microscopy recording the adhesion of EcM1*lux*SAgfp bacteria to HeLa-GFP-tm cells, selecting a field in the microscope that allow comparison of the behavior of bacteria encountering antigen-positive and antigen-negative cells. For this experiment infection of HeLa-GFP-tm culture was performed with a lower MOI (100:1) to reduce bacteria in the medium that could hinder the visualization of cells. The result from this experiment (Supplementary Video 2) showed that antigen-positive HeLa-GFP-tm cells (green) were covered with bacteria within 5 min, whereas almost no bacteria were attached to antigen-negative cells. Interestingly, a significant number of bacteria attached in just 2 min to antigen-positive cells. In fact, adhesion of an individual bacterium occurs in a very short time period (<30 s) after an apparent random collision of a swimming bacterium with the surface of a mammalian cell. After this initial contact with the target cell, bacteria can be observed moving and tumbling in close proximity to the surface of the mammalian cell, eventually establishing a permanent adhesion phenotype and stopping its active motility. In contrast, bacteria that contact with an antigen-negative cell move and tumble close to the cell surface but then swim in a different direction away from the cell (see Supplementary Video 2). This behavior suggests that a productive adhesion of the SAs to the target surface is somehow transduced by the bacterium to stop flagella. Interestingly, an arrest of flagellum rotation has been described in the adhesion of *Caulobacter crescentus* to surfaces during its life cycle.[30] In *E. coli*, intracellular levels of c-di-GMP second messenger have been proposed to regulate changes in flagellar rotation during the transition between motile and surface-attached multicellular communities.[31] Taken together, our experiments demonstrated that the engineered *E. coli* strains with constitutive expression of SAs were able to adhere fast, in high numbers, and in a highly specific manner to mammalian cells expressing on their surface the target antigen recognized by the SA. In addition, the mechanisms underlying the behavior of engineered *E. coli* with SAs to a target surface might be related to those found in natural adhesion processes that trigger arrest of flagellar rotation.

Colonization of Tumors *in Vivo* by Engineered *E. coli* with Synthetic Adhesins. To test the functionality of the SAs *in vivo*, we evaluated whether the engineered bacteria exhibited an improved colonization of solid tumors expressing the target antigen on the surface of tumor cells. It is well established from animal models and clinical trials that intravenous administration of facultative anaerobic bacteria such as *Salmonella* and *E. coli* strains results in the preferential bacterial colonization of solid tumors.[32] This natural ability of anaerobic bacteria for tumor colonization has encouraged research aimed to engineer the expression of therapeutic proteins within the tumor (e.g., cytotoxins, pro-drug converting enzymes) as well as gene reporters for *in vivo* tumor diagnosis (e.g., bioluminescence, magnetic resonance imaging).[32,33] Clinical trials using systemic administration of *Salmonella* for human cancer therapy revealed that the highest bacterial dose that was tolerated was still insufficient for the effective colonization of solid tumors found in those patients.[34,35] Therefore, it would be of interest to engineer bacteria with improved tumor colonization capabilities (i.e., requiring lower doses of administered bacteria and showing an increased ratio of bacteria in tumors versus healthy organs).[32]

It has been previously shown that systemic administration of a single bacterial dose of 5×10^6 CFU of wild type *E. coli* K-12 (strain MG1655) to tumor-bearing mice elicited colonization of >90% of the tumors.[9] Three to 5 days after its intravenous injection, *E. coli* K-12 bacteria were recovered in high numbers from the tumor mass ($\sim 10^8$ CFU/g), whereas organs such as liver or spleen had low bacterial numbers ($<10^3$ CFU/g). Following a similar approach, we established an *in vivo* tumor xenograft model based on HeLa-GFP-tm cells. Athymic Nude mice that received subcutaneously $\sim 10^6$ HeLa-GFP-tm cells developed solid tumors of ~200−400 mm^3 in about 10−15 days. These animals were divided in two experimental groups ($n = 6$) and received intravenously in their lateral tail vein a single dose of 1×10^7 CFU of EcM1*lux*SAtir or EcM1*lux*SAgfp. Four days after the intravenous injection, live imaging of the animals showed bioluminescence signals in the tumors from both groups, and bacteria were found in high numbers ($\sim 10^8$−10^9 CFU/g) in all tumors from each group (6/6) (Supplementary Figure S5a), whereas livers and spleens did not contain bacteria (detection limit $\sim 5 \times 10^1$ CFU/g) or had low bacterial numbers ($<10^3$ CFU/g) (Supplementary Figure S5b). The level of expression of the SAs and bioluminescence signals were identical in the inoculated bacteria and in tumor-recovered bacteria, showing the stability of the expression of SAs *in vivo* (Supplementary Figure S6). Histological cross sections of colonized HeLa-GFP-tm tumors stained with anti-*E. coli* antibodies revealed that bacteria from both strains localized preferentially at inner regions of the tumors (Supplementary Figure S7), especially at the border with outer regions where tumor cells preferentially proliferate. A similar pattern of bacterial distribution was reported for tumors colonized with wild type *E. coli* MG1655.[9]

Hence, the above data indicated that the engineered *E. coli* strains stably expressed the SAs *in vivo* and maintained the capacity to colonize solid tumors of HeLa-GFP-tm cells regardless of the specificity of the SA when a high bacterial dose was administered (1×10^7 CFU). To determine whether SAs could favor tumor colonization with lower bacterial doses, first we showed that a bacterial dose of 1×10^5 CFU was suboptimal for the colonization of HeLa-GFP-tm tumors by wild type *E. coli* MG1655 as only one-third of the tumors (3/9) were colonized 4 days after its systemic administration (Figure 4a). This dose represents 2% of the dose reported for optimal tumor colonization with wild type *E. coli* MG1655.[9] Nevertheless, those tumors that were colonized had bacterial titers ($\sim 10^8$ CFU/g) similar to those found with high bacterial doses, suggesting that once *E. coli* succeeded at an early stage of tumor colonization, bacteria can proliferate, reaching a final titer that is independent of the inoculated dose. In contrast, livers and

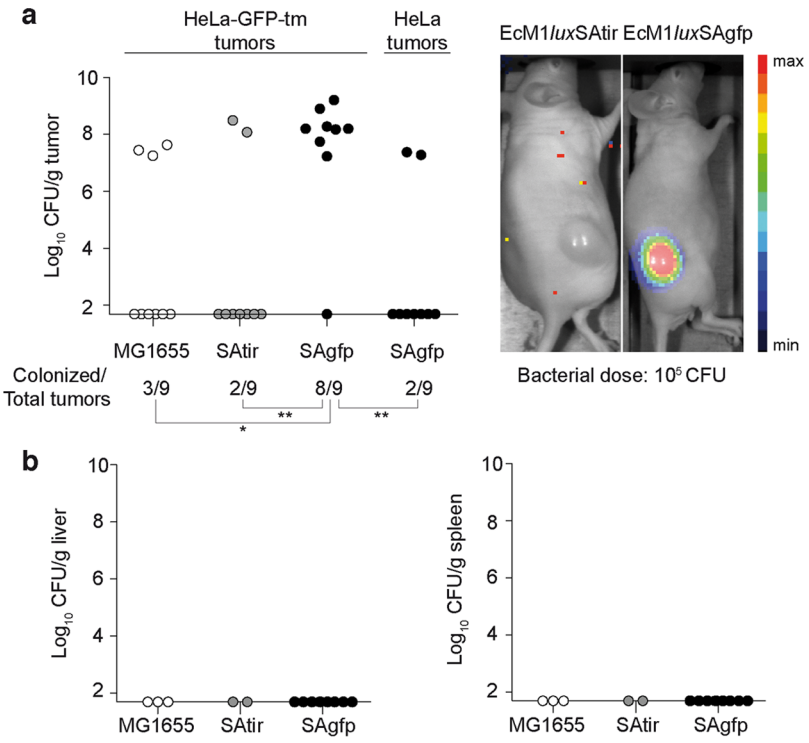

Figure 4. *In vivo* colonization of tumors with low doses of *E. coli* expressing synthetic adhesins. (a) Bacterial colonization of HeLa-GFP-tm or HeLa tumors, as indicated on top, by the following *E. coli* strains: wild type K-12 (MG1655), EcM1*lux*SAtir (SAtir), and EcM1*lux*SAgfp (SAgfp). Each bacterial strain was intravenously administered (1×10^5 CFU/mouse) to tumor-bearing mice (experimental groups $n = 9$) and 4-days postadministration the number of CFU in each tumor was determined. Each circle in the graph represents the CFU determined per gram of tumor (Log_{10} CFU/g) for each animal in the different experimental groups. The ratio of colonized tumors in each group is shown at the bottom along with the statistical analyses between groups connected with lines. Two-tailed *P* values of Fisher's exact test are indicated with one asterisk (*) when $P < 0.05$ or two asterisks (**) when $P = 0.015$. On the right, bioluminescence live imaging of HeLa-GFP-tm tumor-bearing mouse infected with 1×10^5 CFU of EcM1*lux*SAtir (left image) or EcM1*lux*SAgfp (right image). Images are overlays of photographic white-light and bioluminescence signals from a representative tumor-bearing mouse infected with the strains, as indicated on top. The intensities of the bioluminescence signals are represented in pseudocolor according to the scale bar. (b) Graphs showing bacterial titers in livers (left) and spleens (right) from those animals with a HeLa-GFP-tm tumor colonized in panel a by wild-type K-12 (MG1655), EcM1*lux*SAtir (SAtir), or EcM1*lux*SAgfp (SAgfp) strains. Each circle in the graph represents the CFU determined per gram of tissue (log_{10} CFU/g).

spleens of these animals had undetectable levels of bacteria (Figure 4b).

Therefore, a suboptimal dose of 1×10^5 CFU was chosen to compare the tumor colonization capacity of the engineered *E. coli* strains. As above, EcM1*lux*SAtir or EcM1*lux*SAgfp bacteria were administered intravenously to two groups of Nude mice ($n = 9$) bearing subcutaneous HeLa-GFP-tm tumors (≥200 mm^3). Four days after inoculation, most animals (8/9) of the group inoculated with EcM1*lux*SAgfp had their tumors colonized with high bacterial titers ($\geq 10^8$ CFU/gr), whereas less than one-third of the animals (2/9) in the group inoculated with EcM1*lux*SAtir had colonized tumors (Figure 4a). This differential colonization was also detected by bioluminescence *in vivo* imaging of the animals (Figure 4a). As a control for specificity, a dose of 1×10^5 CFU of EcM1*lux*SAgfp strain was also administered systemically to a group ($n = 9$) of Nude mice bearing tumors derived from untransfected HeLa cells. Four days after inoculation, HeLa tumors were colonized with low efficiency (2/9) by EcM1*lux*SAgfp strain, identical to that found with EcM1*lux*SAtir strain in HeLa-GFP-tm tumors (Figure 4a). In addition, livers and spleens of animals with colonized tumors had undetectable levels of bacteria (Figure 4b). Taken together, these results demonstrated that engineered *E. coli* with SAs were able to colonize solid tumors expressing a target cell surface antigen with high efficiency and specificity using low bacterial doses that are suboptimal for wild type *E. coli* or engineered bacteria with a SA of a different specificity.

Several factors have been proposed to be involved in the colonization of solid tumors by *E. coli* and other facultative and anaerobic bacteria (e.g., *Salmonella*, *Listeria*, *Bifidobacterium*). The initial bacterial entry seems to be due to the highly permeable and abnormal vasculature of the tumor.[36] Infecting bacteria also induce pro-inflammatory signals (e.g., tumor necrosis factor α; TNFα) that increase blood flooding into the tumor mass assisting bacterial entry.[37] At this stage, bacterial adhesion to tumor cells mediated by SAs may facilitate successful tumor colonization. At later stages, bacterial replication is favored in the intratumoral microenvironment, rich in certain nutrients (e.g., amino acids, ribose) and having a low oxygen concentration that impairs clearance of bacteria by the immune system.[32] In the colonized tumors, we found similar bacterial titers and intratumoral distribution irrespective of the specificity of the SA or antigen expressed by the tumor, indicating that SAs appear to have less influence in the replication and intratumoral distribution of bacteria at a later stage of the colonization.

Lower Retention of Engineered *E. coli* in Liver and Spleen. Next, we investigated whether the engineered bacteria with SAs and lacking natural adhesins, in addition to the

dx.doi.org/10.1021/sb500252a | *ACS Synth. Biol.* 2015, 4, 463−473

improved colonization of target tumors shown previously, could have a lower retention in normal organs compared to wild type *E. coli*. For this purpose, we analyzed bacterial titers in livers and spleens of two groups (n = 9) of Nude mice without implanted tumors in which a high dose (1×10^7 CFU) of wild type *E. coli* MG1655 or engineered EcM1*lux*SAgfp was inoculated. Three mice from each group were euthanized at 4, 24, and 48 h after inoculation, and the bacterial titers in liver and spleen were determined (Figure 5). This experiment

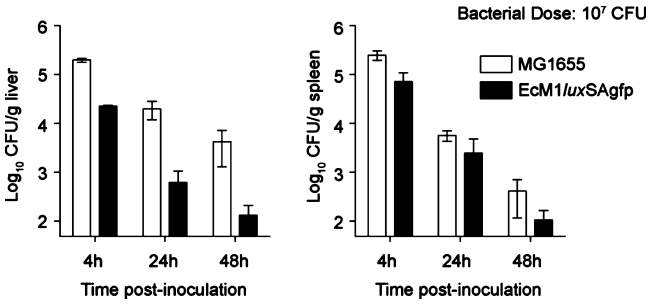

Figure 5. Low retention of the engineered *E. coli* strain in healthy organs. Bacterial titers ($\log_{10}$ CFU/g) recovered from livers (left) and spleens (right) of tumor-less Nude mice at 4, 24, and 48 h after intravenous administration of 1×10^7 CFU of wild type *E. coli* K-12 (MG1655) or EcM1*lux*SAgfp, as indicated. Each bar represents the average CFU/g with standard deviation determined from three mice from each group at the indicated time postinoculation.

revealed that, at all the time points analyzed, the titers of the engineered *E. coli* strain in these organs were lower than those in the case of the wild type *E. coli* strain, especially in liver where the titers of engineered bacteria were ~10−30 times lower than the wild type strain (Figure 5). In the spleen, the engineered bacteria had titers ~2−4-fold lower than the wild type strain. Therefore, these data indicate that the engineered bacteria exhibit a lower retention in healthy organs than the wild type *E. coli* strain. This phenotype might be due to the deletion of natural adhesins in the engineered strain (i.e., type 1 fimbriae, Antigen 43, and MAT fimbriae) that have the potential to bind receptors widely expressed in the surface of multiple host cells and tissues.[11,24] Hence, expression of SAs into an *E. coli* chassis lacking of a set of natural adhesins generates bacteria with selective adhesion to target tissues and lower adhesion to non-target organs.

Conclusions. We have engineered a stable and specific adhesion of *E. coli* bacteria with SAs based on the β-domain from intimin[12] and the Ig-domain from VHHs.[14] Constitutive expression of SAs from the chromosome did not affect growth and viability of the engineered *E. coli* strain, being stably maintained through multiple generations without selection pressure. The modular architecture of the SAs makes possible the simple modification of their specificity by an exchange of the VHH sequence, which can be selected from repertoires employing phage and cell display technologies.[14,15] This could allow the generation of SAs against virtually any antigen of interest, enabling the design of *E. coli* targeting any chosen surface or cell. In addition, intimin β-domain and VHHs are resistant to proteases and denaturant agents (e.g., SDS, urea, temperature).[13,14] Altogether, these properties make SAs extremely robust, inducing the stable attachment of a great number of *E. coli* bacteria to the targeted surface or cell. Furthermore, we have demonstrated the functionality of SAs *in vivo* showing that the engineered *E. coli* strain colonizes more efficiently solid tumors expressing a target antigen. The higher efficiency introduced by the SAs allowed a significant reduction (ca. 2 orders of magnitude) of the bacterial dose needed for optimal tumor colonization *in vivo*, an important issue in order to increase the biosafety of bacterial therapies.[32] Tumors cells often deregulate the expression and/or post-translational modification of cell surface proteins (e.g., growth factor receptors, mucins), which has been used as targets for developing therapeutic antibodies against tumor cells.[38,39] Hence, SAs against these validated targets could improve bacterial colonization of specific tumors.

Engineered *E. coli* expressing SAs may be of interest for other biomedical and industrial applications. For instance, SAs could help in the localized delivery of antigens to specific immune cells for more effective vaccines based on bacterial vectors.[40] SAs could also be targeted to antigens expressed by viral and bacterial pathogens, which could facilitate the therapeutic intervention of engineered bacteria against pathogens.[41,42] In addition, targeting of other bacteria could generate defined bacterial consortia for industrial bioprocesses,[43] whereas adhesion to abiotic surfaces could improve the development of biosensors.[44] Given the conservation of the cellular machineries used for folding and insertion of β-barrel OM proteins,[45,46] it is likely that the reported SAs of *E. coli* could be functional in other Gram-negative bacterial species, including alternative nonpathogenic bacteria used in synthetic biology such as *Pseudomonas putida*.[47] In conclusion, SAs could be applied in multiple synthetic biology projects, and future work should expand their use in *E. coli* and other bacteria for specialized applications.

METHODS

Bacterial Strains and Growth Conditions. The *E. coli* strains used in the experiments described in this work are listed in Supplementary Table S1. Bacteria were grown in Luria−Bertani (LB) liquid medium and agar plates (1.5% w/v), at 37 °C, unless otherwise indicated. When needed for plasmid or strain selection, antibiotics were added to the media at the following concentrations: chloramphenicol (Cm) at 30 μg/mL, ampicillin (Ap) at 100 μg/mL, and kanamycin (Km) at 50 μg/mL. *E. coli* DH10B-T1^R strain was used as host for cloning and propagation of plasmids with a pBR origin of replication (e.g., pAK-Not, pNV-derivatives). For cloning and propagation of suicide pGE-plasmid derivatives, containing the conditional pi-dependent R6K origin of replication,[48] the *E. coli* strains BW25141 or CC118-λpir were used. For inducible expression of the SAs from plasmid vectors with *plac* promoter (i.e., pNVfib, pNVgfp), EcM1 bacteria bearing the corresponding plasmid were grown in LB-Cm at 30 °C, and 0.05 mM isopropyl-thio-β-D-galactoside (IPTG) was added at an optical density 600 nm (OD_{600}) of 0.5. The cultures were further grown for 2 h at 30 °C with agitation (160 rpm). Bacteria with constitutive expression of the synthetic adhesins and the *lux* operon from the chromosome were always grown statically at 37 °C in LB, except for analysis of their growth curve in which cultures were grown at 37 °C with agitation (160 rpm). Bioluminescence of bacterial colonies grown on LB plates were monitored in a Chemi-doc XRS+ (Bio-Rad).

Plasmids, DNA Constructs, and Oligonucleotides. The plasmids constructed and used in this study are summarized in Supplementary Table S1. Oligonucleotides were synthesized by Sigma Genosys and are listed in Supplementary Table S2. PCRs were performed with Taq DNA polymerase for standard

dx.doi.org/10.1021/sb500252a | ACS Synth. Biol. 2015, 4, 463−473

amplifications in screenings and with proof-reading DNA polymerases, Vent DNA polymerase (New England Biolabs) and High-expand fidelity (Roche) for cloning purposes. All plasmid constructs were fully sequenced (Secugen). Details of plasmid constructions are described as Supporting Information.

E. coli Genome Modification and Strain Construction. Site-specific deletions and insertions in the chromosome of *E. coli* were done with the marker-less strategy of genome edition based on expression of I-SceI endonuclease.[4,21] Briefly, the *E. coli* strain to be modified was initially transformed with plasmid pACBSR (Cm^R),[49] expressing I-SceI and λ Red proteins under the control of P_{BAD} promoter (inducible with L-arabinose), and subsequently electroporated with the corresponding pGE-based suicide vector (Km^R). Cointegrants were selected on LB-Cm-Km plates incubated at 37 °C. Individual colonies were isolated and grown for 6 h in LB-Cm liquid medium containing L-arabinose 0.4% (w/v) with agitation (160 rpm). After this period, a ∼1 μL sample of these cultures was streaked on LB-Cm plates using an inoculating loop and incubated overnight. Individual colonies were replicated in LB-Cm and LB-Cm-Km plates to screen for Km-sensitive colonies that have performed resolution of the cointegrant vector after I-SceI induction. Individual Km-sensitive colonies were screened by PCR with specific oligonucleotides to identify those with the desired modification in their chromosome (i.e., deletion, insertion, substitution). Plasmid pACBSR was cured from the final strain by growth in liquid LB and streaking on LB plates. Individual colonies were replicated in LB and LB-Cm plates to screen for Cm-sensitive colonies. Construction details of individual *E. coli* strains are described as Supporting Information.

***In Vitro* Cell Culture and Plasmid Transfection.** The human epithelial tumor cell line HeLa (ATCC, CCL-2) was grown as a monolayer in Dulbecco's modified Eagle's medium (DMEM), supplemented with 10% fetal bovine serum (FBS) and 2 mM glutamine (complete DMEM), at 37 °C with 5% CO_2. For transfection, HeLa cells were seeded in 24-well tissue culture plates (BD Falcon) (∼10^5 cells/well), grown for 20 h at 37 °C with 5% CO_2, and transfected with 0.6 μg/well of plasmids pDisplay-GFP-tm or pDisplay-TirM-tm following the calcium phosphate method.[50] After 22 h incubation at 37 °C with 5% CO_2, the medium was removed, and wells were washed three times with phosphate-buffered saline (PBS) and filled with complete DMEM medium containing G418 (0.5 mg/mL, Invitrogen, Life Technologies). After 24 h incubation, cells were passed to a T75 flask (BD Falcon) with the same medium and further grown. G418-resistant HeLa cells expressing GFP or mWasabi fusion proteins were selected from these cultures by fluorescence activated cell sorting (FACS) using an Epics-Altra Cell Sorter (Beckman Coulter). HeLa-GFP-tm and HeLa-TirM-tm positive cells populations were expanded on complete DMEM medium.

Flow Cytometry Analysis. Bacteria (equivalent to a final OD_{600} of 1.0) were harvested from cultures by centrifugation (4000 × *g*, 3 min), washed with PBS, and resuspended in 1 mL of PBS containing 10% (v/v) goat serum (Sigma). An aliquot sample of 200 μL was incubated for 1 h on ice with anti-myc mAb clone 9B11 (1:200; Cell Signaling Technology). Next, bacteria were washed in PBS, resuspended in 500 μL of PBS containing 10% (v/v) goat serum, and stained for 40 min in the dark with Alexa 488-conjugated anti-mouse IgGs (1:500; Molecular Probes, Life Technologies). Bacteria were finally washed and resuspended in a final volume of 1 mL of PBS and analyzed in a flow cytometer (Gallios, Beckman Coulter).

Protein Extract Preparation, SDS-PAGE, and Western Blots. Whole-cell protein extracts were prepared in urea-SDS sample buffer as described previously.[13] SDS-polyacrylamide gel electrophoresis (PAGE) and immunoblotting conditions to polyvinylidene difluoride membrane (PVDF, Immobilon-P; Millipore) have been reported.[13,15] For immunodetection, the PVDF membranes were incubated with anti-myc mAb clone 9B11 (1:2000; Cell Signaling Technology) to detect myc-tagged SAs and anti-mouse IgG-peroxidase (POD) conjugate (1:5000; Sigma) as secondary antibody. GroEL was detected with anti-GroEL mAb-POD conjugate (1:5000; Sigma). Membranes were developed by chemiluminescence using a mixture in 100 mM Tris-HCl (pH 8.0) containing 1.25 mM luminol (Sigma), 0.22 mM cumaric acid (Sigma), and 0.0075% (v/v) H_2O_2 (Sigma) and exposed to an X-ray film (Curix, Agfa).

Adhesion Assays to Antigens Immobilized on a Plastic Surface. Purified GFP (Upstate, Millipore) or human fibrinogen (Enzyme Research Laboratories) as indicated was diluted in PBS to 10 μg/mL, and 100 μL was adsorbed onto ELISA plates (Maxisorb, Nunc) overnight at 4 °C. Antigen-coated plates were washed with PBS and blocked for 1 h at room temperature with PBS containing 3% (w/v) skimmed milk. Next, a bacterial suspension (100 μL) of the indicated strain was added at an OD_{600} of 3.0 in PBS and incubated for an additional 1 h. The plates were then washed with PBS three times, and the presence of bound bacteria was visualized by light microscopy and macroscopically detected by staining with crystal violet solution (Sigma).

Adhesion Assays to *in Vitro* Cultured HeLa Cells and Immunofluorescence Microscopy. Bacteria of the indicated *E. coli* strain were harvested by centrifugation (4000 × *g*, 3 min) from static liquid LB cultures grown overnight at 37 °C. An OD_{600} of 1.0 from these cultures grown statically was determined to contain ∼3 × 10^8 CFU/mL by plating in LB agar. Bacteria were washed in PBS and resuspended at 3 × 10^7 CFU/mL in PBS or DMEM. For an infection at MOI 300:1, a 1 mL sample of this bacterial suspension was added to a single well of a 24-well tissue culture plate having the indicated HeLa cell line (∼10^5 cells/well). HeLa cells were grown on sterile coverslips (13 mm diameter, VWR international) placed at the bottom of the well. After 1 h infection at 37 °C, the wells were aspirated and washed five times with 1 mL of PBS at room temperature. The coverslips were fixed for 20 min at room temperature with 0.5 mL of a paraformaldehyde 4% (w/v) solution in PBS and washed three times with 1 mL of PBS. Coverslips were blocked and stained for 1 h at room temperature in a wet chamber with 50 μL of PBS/10% goat serum solution having a rabbit polyclonal serum anti-*E. coli* O and K antigenic serotypes (1:1000; Biodesign). The coverslips were washed by immersion 15 times in a large volume of PBS (100 mL), placed again the wet chamber, and incubated for 40 min at room temperature with 50 μL of PBS/10% goat serum solution having a goat anti-rabbit IgG-Alexa 594 conjugated secondary antibody (1:500; Molecular Probes, Life Technologies) and DAPI (1:500; Sigma). Next, the coverslips were washed with PBS as above, the excess of liquid was removed by touching a kimwipe with the edge of the coverslip, and the coverslips were mounted with 2 μL of Prolong (Invitrogen) on glass slides. The samples were examined by epifluorescence microscopy (Zeiss Axio imager microscope) or by confocal microscopy (Leica TCS SP5 multispectral confocal system). For time-lapse live cell video microscospy, HeLa-GFP-tm cells,

grown on 24-well tissue culture plates, were infected with 1×10^7 CFU of EcM1*lux*SAgfp in a final volume ~0.3 mL/well (MOI 100:1) and monitored using an Olympus IX71 microscope equipped with an Olympus cell^R motorized TIRF system.

Infection of Tumor-Bearing Mice and Recovery of Bacteria from Tissues. All animals experiments were done in accordance with protocols approved by the CNB Ethics Committee for Animal Experimentation (ref 11034) and by the Hospital Universitario Puerta de Hierro Animal Care and Use Committee, in compliance with Spanish and European Union legislation. Five-week-old athymic female Hsd:Athymic Nude-*Foxn1*^{nu} were obtained from Harlan (Harlan Ibérica). Tumor-bearing mice were generated by subcutaneous injection of ~1×10^6 HeLa-GFP-tm or HeLa cells, as indicated, in 100 μL of PBS containing 20% (v/v) Matrigel (BD Biosciences), into the abdominal right flank of 6-week-old Nude mice. Tumor volumes were estimated with calipers according to the formula: width^2 × length × 0.52. When tumors reached a volume between 200 and 400 mm^3, the mice were randomly divided into experimental groups. Bacteria were grown and harvested as described above for the *in vitro* adhesion assays and resuspended in sterile PBS at 1×10^8 CFU/mL. For each independent experiment the number of CFU in this bacterial suspension was determined, showing an experimental error below 10%. This bacterial stock was directly used for systemic inoculation of mice receiving a dose of 1×10^7 CFU by injection of 100 μL into the lateral tail vein using a 0.5 mL syringe with a 29G needle (Becton Dickinson). Alternatively, for mice receiving a dose of 1×10^5 CFU, the original bacterial stock was diluted in PBS to 1×10^6 CFU/mL, and 100 μL was injected per mouse as above. These bacterial doses did not cause any apparent disease symptoms in the animals, which showed normal phenotype throughout the entire experiment (i.e., mobility, weight, feeding behavior). For determination of bacterial CFU per gram (CFU/g) of tumors, livers, and spleens, animals were euthanized, and tumors and organs were excised, placed individually into (preweighed) sterile tubes containing 5 mL of PBS, and weighed. Samples were then transferred to sterile sampling bags (VWR), and Triton X-100 (Sigma) was added to a final concentration of 0.2% (v/v). Samples were homogenized by soft mechanical squeezing. Next, a 100-μL sample of the homogenates was serially diluted in LB, plated in LB agar, and incubated overnight at 37 °C to determine CFU. Bacterial titers were expressed as CFU/g of tissue. For statistical analysis a minimal bacterial titer of 50 CFU/g, corresponding to the detection limit of the assay, was considered in those cases in which no bacteria were detected by plating.

Bioluminescence Imaging. Bacterial light emission from LB plates or from tissue culture plates was captured using a ChemiDoc XRS system (Bio-Rad). For live imaging of bioluminescent bacteria in tumor-bearing mice, animals were anesthetized with 4% Isoflurane (Forene, Abbott) and maintained under 1% Isoflurane in a thermostated chamber with a high-resolution charge-coupled-device (CCD) cooled digital camera ORCA-2BT (Hamamatsu Photonics). Imaging analysis was done with the Hokawo software (Hamamatsu Photonics).

Statistics. Statistical analyses comparing the ratio of colonized tumors between experimental groups were conducted with Fisher's exact test to determine two-tailed *P* values using Prism 5.0 (GraphPad software Inc.). Data were considered significantly different when $P < 0.05$.

Histology. For *ex vivo* histological analyses, resected tumors were fixed with 4% (w/v) paraformladehyde in PBS for 16 h at 4 °C and embedded in paraffin. Serial 6 μm sections were cut at the tumor center with a microtome (Leica RM2155) and placed onto glass slides. The samples were deparaffinized with xylene and ethanol solutions, rehydrated in PBS, and incubated with 1 M citrate buffer (pH 6.0) and PBS-Tween (PBS, 0.1% Tween 20) to unmask antigens. Tissue sections were blocked with 10% goat serum in PBS-Tween and incubated with anti-*E. coli* polyclonal serum (1:100) 1 h at room temperature in the same buffer. Next, samples were washed with PBS-Tween and incubated with goat anti-rabbit IgG-Alexa 594 conjugated secondary antibody (1:500) in PBS-Tween with 10% goat serum for 1 h at room temperature. Samples were mounted in Vectashield media (Vector Laboratories), and images were obtained with a fluorescence microscope (Leica DMI6000B fluorescence system with Orca R^2 digital camera from Hamamatsu).

■ ASSOCIATED CONTENT

Supporting Information

Contains further details about plasmid and bacterial strain constructions, supplemental tables, references and figures. Video 1: Sequential Z stack images of HeLa-GFP-tm cells infected with EcM1*lux*SAgfp bacteria (MOI 300:1) obtained by confocal laser scanning microscopy. After 1 h of infection, cells and bacteria were fixed with paraformaldehyde. Mammalian cells expressing GFP (green) and bacteria (red) were labeled with anti-*E. coli* rabbit polyclonal antibodies and anti-rabbit-Alexa-594 antibodies. The bacterial and cellular genomes (blue) were stained with DAPI. Video 2. Infection of HeLa-GFP-tm cells with EcM1*lux*SAgfp bacteria (MOI 100:1) assessed by time-lapse live-cell video microscopy using an Olympus IX71 microscope equipped with an Olympus motorized CellR^TIRF system. Addition of bacteria to the culture started at 00:00:27 s, and images were acquired for 5 min. This material is available free of charge via the Internet at http://pubs.acs.org.

■ AUTHOR INFORMATION

Corresponding Author

*Phone: +34 91 585 48 54. Fax: +34 91 585 45 06. E-mail: lafdez@cnb.csic.es.

Author Contributions

§These authors contribute equally to this work.

Notes

The authors declare no competing financial interest.

■ ACKNOWLEDGMENTS

We thank Prof. Víctor de Lorenzo for valuable discussion and support. We especially thank the excellent technical assistance of Sylvia Gutiérrez Erlandsson (Confocal Microscopy facility of the CNB) and Francisco Javier Martin Torre (Animal House facility of the CNB). Work in the laboratory of LAF is supported by research grants from the Spanish "Ministerio de Economía y Competitividad" (MINECO) (BIO2011-26689), "Comunidad Autónoma de Madrid" (S2010-BMD-2312), "La Caixa" Foundation, and the European Research Council (ERC-2012-ADG_20120314). C.P.-L. was supported by a Ph.D. FPI contract BES-2009-024051 from MINECO. Work in the laboratory of L.A.-V. is supported by research grants from

MINECO (BIO2011-22738) and "Comunidad Autónoma de Madrid" (S2010-BMD-2312). R.F.-P. was supported by a Ph.D. FPI contract BES-2009-027649 from MINECO.

REFERENCES

(1) Khalil, A. S., and Collins, J. J. (2010) Synthetic biology: applications come of age. *Nat. Rev. Genet. 11*, 367−379.
(2) Korea, C. G., Ghigo, J. M., and Beloin, C. (2011) The sweet connection: Solving the riddle of multiple sugar-binding fimbrial adhesins in *Escherichia coli*: Multiple *E. coli* fimbriae form a versatile arsenal of sugar-binding lectins potentially involved in surface-colonisation and tissue tropism. *Bioessays 33*, 300−311.
(3) Kline, K. A., Falker, S., Dahlberg, S., Normark, S., and Henriques-Normark, B. (2009) Bacterial adhesins in host-microbe interactions. *Cell Host Microbe 5*, 580−592.
(4) Posfai, G., Plunkett, G., 3rd, Feher, T., Frisch, D., Keil, G. M., Umenhoffer, K., Kolisnychenko, V., Stahl, B., Sharma, S. S., de Arruda, M., Burland, V., Harcum, S. W., and Blattner, F. R. (2006) Emergent properties of reduced-genome *Escherichia coli*. *Science 312*, 1044−1046.
(5) Huang, C. J., Lin, H., and Yang, X. (2012) Industrial production of recombinant therapeutics in *Escherichia coli* and its recent advancements. *J. Ind. Microbiol. Biotechnol. 39*, 383−399.
(6) Tenaillon, O., Skurnik, D., Picard, B., and Denamur, E. (2010) The population genetics of commensal *Escherichia coli*. *Nat. Rev. Micrbiol. 8*, 207−217.
(7) Salvador, E., Wagenlehner, F., Kohler, C. D., Mellmann, A., Hacker, J., Svanborg, C., and Dobrindt, U. (2012) Comparison of asymptomatic bacteriuria *Escherichia coli* isolates from healthy individuals versus those from hospital patients shows that long-term bladder colonization selects for attenuated virulence phenotypes. *Infect. Immun. 80*, 668−678.
(8) Sonnenborn, U., and Schulze, J. (2009) The non-pathogenic *Escherichia coli* strain Nissle 1917−features of a versatile probiotic. *Microb. Ecol. Health Dis. 21*, 122−158.
(9) Weibel, S., Stritzker, J., Eck, M., Goebel, W., and Szalay, A. A. (2008) Colonization of experimental murine breast tumours by *Escherichia coli* K-12 significantly alters the tumour microenvironment. *Cell. Microbiol. 10*, 1235−1248.
(10) Stritzker, J., Weibel, S., Hill, P. J., Oelschlaeger, T. A., Goebel, W., and Szalay, A. A. (2007) Tumor-specific colonization, tissue distribution, and gene induction by probiotic *Escherichia coli* Nissle 1917 in live mice. *Int. J. Med. Microbiol. 297*, 151−162.
(11) Bodelón, G., Palomino, C., and Fernández, L. A. (2013) Immunoglobulin domains in *Escherichia coli* and other enterobacteria: from pathogenesis to applications in antibody technologies. *FEMS Microbiol. Rev. 37*, 204−250.
(12) Fairman, J. W., Dautin, N., Wojtowicz, D., Liu, W., Noinaj, N., Barnard, T. J., Udho, E., Przytycka, T. M., Cherezov, V., and Buchanan, S. K. (2012) Crystal structures of the outer membrane domain of intimin and invasin from enterohemorrhagic *E. coli* and enteropathogenic *Y. pseudotuberculosis*. *Structure 20*, 1233−1243.
(13) Bodelón, G., Marín, E., and Fernández, L. A. (2009) Role of periplasmic chaperones and BamA (YaeT/Omp85) in folding and secretion of Intimin from enteropathogenic *Escherichia coli* strains. *J. Bacteriol. 191*, 5169−5179.
(14) Muyldermans, S. (2013) Nanobodies: natural single-domain antibodies. *Annu. Rev. Biochem. 82*, 775−797.
(15) Salema, V., Marín, E., Martínez-Arteaga, R., Ruano-Gallego, D., Fraile, S., Margolles, Y., Teira, X., Gutierrez, C., Bodelón, G., and Fernández, L. Á. (2013) Selection of single domain antibodies from immune libraries displayed on the surface of *E. coli* cells with two β-domains of opposite topologies. *PLoS One 8*, e75126.
(16) Francisco, J. A., Campbell, R., Iverson, B. L., and Georgiou, G. (1993) Production and fluorescence-activated cell sorting of *Escherichia coli* expressing a functional antibody fragment on the external surface. *Proc. Natl. Acad. Sci. U.S.A. 90*, 10444−10448.
(17) Marín, E., Bodelón, G., and Fernández, L. A. (2010) Comparative analysis of the biochemical and functional properties of C-terminal domains of autotransporters. *J. Bacteriol. 192*, 5588−5602.
(18) Georgiou, G., Stephens, D. L., Stathopoulos, C., Poetschke, H. L., Mendenhall, J., and Earhart, C. F. (1996) Display of beta-lactamase on the *Escherichia coli* surface: outer membrane phenotypes conferred by Lpp'-OmpA'-beta-lactamase fusions. *Protein Eng. 9*, 239−247.
(19) Leyton, D. L., Rossiter, A. E., and Henderson, I. R. (2012) From self sufficiency to dependence: mechanisms and factors important for autotransporter biogenesis. *Nat. Rev. Microbiol 10*, 213−225.
(20) Connell, I., Agace, W., Klemm, P., Schembri, M., Marild, S., and Svanborg, C. (1996) Type 1 fimbrial expression enhances *Escherichia coli* virulence for the urinary tract. *Proc. Natl. Acad. Sci. U.S.A. 93*, 9827−9832.
(21) Posfai, G., Kolisnychenko, V., Bereczki, Z., and Blattner, F. R. (1999) Markerless gene replacement in *Escherichia coli* stimulated by a double-strand break in the chromosome. *Nucleic Acids Res. 27*, 4409−4415.
(22) Frankel, G., Phillips, A. D., Trabulsi, L. R., Knutton, S., Dougan, G., and Matthews, S. (2001) Intimin and the host cell—is it bound to end in Tir(s)? *Trends Microbiol. 9*, 214−218.
(23) Deuschle, U., Kammerer, W., Gentz, R., and Bujard, H. (1986) Promoters of *Escherichia coli*: a hierarchy of in vivo strength indicates alternate structures. *EMBO J. 5*, 2987−2994.
(24) van der Woude, M. W., and Henderson, I. R. (2008) Regulation and function of Ag43 (flu). *Annu. Rev. Microbiol. 62*, 153−169.
(25) Winson, M. K., Swift, S., Hill, P. J., Sims, C. M., Griesmayr, G., Bycroft, B. W., Williams, P., and Stewart, G. S. (1998) Engineering the *luxCDABE* genes from *Photorhabdus luminescens* to provide a bioluminescent reporter for constitutive and promoter probe plasmids and mini-Tn5 constructs. *FEMS Microbiol. Lett. 163*, 193−202.
(26) Rendon, M. A., Saldana, Z., Erdem, A. L., Monteiro-Neto, V., Vazquez, A., Kaper, J. B., Puente, J. L., and Giron, J. A. (2007) Commensal and pathogenic *Escherichia coli* use a common pilus adherence factor for epithelial cell colonization. *Proc. Natl. Acad. Sci. U.S.A. 104*, 10637−10642.
(27) Chudakov, D. M., Matz, M. V., Lukyanov, S., and Lukyanov, K. A. (2010) Fluorescent proteins and their applications in imaging living cells and tissues. *Physiol. Rev. 90*, 1103−1163.
(28) Ai, H. W., Olenych, S. G., Wong, P., Davidson, M. W., and Campbell, R. E. (2008) Hue-shifted monomeric variants of Clavularia cyan fluorescent protein: identification of the molecular determinants of color and applications in fluorescence imaging. *BMC Biol. 6*, 13.
(29) Rothbauer, U., Zolghadr, K., Muyldermans, S., Schepers, A., Cardoso, M. C., and Leonhardt, H. (2008) A versatile nanotrap for biochemical and functional studies with fluorescent fusion proteins. *Mol. Cell. Proteomics 7*, 282−289.
(30) Kirkpatrick, C. L., and Viollier, P. H. (2012) Reflections on a sticky situation: how surface contact pulls the trigger for bacterial adhesion. *Mol. Microbiol. 83*, 7−9.
(31) Fang, X., and Gomelsky, M. (2010) A post-translational, c-di-GMP-dependent mechanism regulating flagellar motility. *Mol. Microbiol. 76*, 1295−1305.
(32) Forbes, N. S. (2010) Engineering the perfect (bacterial) cancer therapy. *Nat. Rev. Cancer 10*, 785−794.
(33) Huh, J. H., Kittleson, J. T., Arkin, A. P., and Anderson, J. C. (2013) Modular design of a synthetic payload delivery device. *ACS Synth. Biol. 2*, 418−424.
(34) Toso, J. F., Gill, V. J., Hwu, P., Marincola, F. M., Restifo, N. P., Schwartzentruber, D. J., Sherry, R. M., Topalian, S. L., Yang, J. C., Stock, F., Freezer, L. J., Morton, K. E., Seipp, C., Haworth, L., Mavroukakis, S., White, D., MacDonald, S., Mao, J., Sznol, M., and Rosenberg, S. A. (2002) Phase I study of the intravenous administration of attenuated *Salmonella typhimurium* to patients with metastatic melanoma. *J. Clin. Oncol. 20*, 142−152.
(35) Heimann, D. M., and Rosenberg, S. A. (2003) Continuous intravenous administration of live genetically modified *Salmonella typhimurium* in patients with metastatic melanoma. *J. Immunother. 26*, 179−180.

(36) Forbes, N. S., Munn, L. L., Fukumura, D., and Jain, R. K. (2003) Sparse initial entrapment of systemically injected *Salmonella typhimurium* leads to heterogeneous accumulation within tumors. *Cancer Res. 63*, 5188−5193.
(37) Leschner, S., Westphal, K., Dietrich, N., Viegas, N., Jablonska, J., Lyszkiewicz, M., Lienenklaus, S., Falk, W., Gekara, N., Loessner, H., and Weiss, S. (2009) Tumor invasion of *Salmonella enterica* serovar Typhimurium is accompanied by strong hemorrhage promoted by TNF-alpha. *PLoS One 4*, e6692.
(38) Sliwkowski, M. X., and Mellman, I. (2013) Antibody therapeutics in cancer. *Science 341*, 1192−1198.
(39) Oliveira, S., Heukers, R., Sornkom, J., Kok, R. J., and van Bergen En Henegouwen, P. M. (2013) Targeting tumors with nanobodies for cancer imaging and therapy. *J. Controlled Release 172*, 607−617.
(40) Bolhassani, A., and Zahedifard, F. (2012) Therapeutic live vaccines as a potential anticancer strategy. *Int. J. Cancer 131*, 1733−1743.
(41) Saeidi, N., Wong, C. K., Lo, T. M., Nguyen, H. X., Ling, H., Leong, S. S., Poh, C. L., and Chang, M. W. (2011) Engineering microbes to sense and eradicate *Pseudomonas aeruginosa*, a human pathogen. *Mol. Syst. Biol. 7*, 521.
(42) Hwang, I. Y., Tan, M. H., Koh, E., Ho, C. L., Poh, C. L., and Chang, M. W. (2013) Reprogramming microbes to be pathogen-seeking killers. *ACS Synth. Biol. 3*, 228−237.
(43) Minty, J. J., Singer, M. E., Scholz, S. A., Bae, C.-H., Ahn, J.-H., Foster, C. E., Liao, J. C., and Lin, X. N. (2013) Design and characterization of synthetic fungal-bacterial consortia for direct production of isobutanol from cellulosic biomass. *Proc. Natl. Acad. Sci. U.S.A. 110*, 14592−14597.
(44) Park, M., Tsai, S. L., and Chen, W. (2013) Microbial biosensors: engineered microorganisms as the sensing machinery. *Sensors 13*, 5777−5795.
(45) Noinaj, N., Kuszak, A. J., Gumbart, J. C., Lukacik, P., Chang, H., Easley, N. C., Lithgow, T., and Buchanan, S. K. (2013) Structural insight into the biogenesis of β-barrel membrane proteins. *Nature 501*, 385−390.
(46) Hagan, C. L., Silhavy, T. J., and Kahne, D. E. (2011) β-Barrel membrane protein assembly by the Bam complex. *Annu. Rev. Biochem. 80*, 189−210.
(47) Martinez-Garcia, E., and de Lorenzo, V. (2011) Engineering multiple genomic deletions in Gram-negative bacteria: analysis of the multi-resistant antibiotic profile of *Pseudomonas putida* KT2440. *Environ. Microbiol. 13*, 2702−2716.
(48) Stalker, D. M., Kolter, R., and Helinski, D. R. (1982) Plasmid R6K DNA replication. I. Complete nucleotide sequence of an autonomously replicating segment. *J. Mol. Biol. 161*, 33−43.
(49) Herring, C. D., Glasner, J. D., and Blattner, F. R. (2003) Gene replacement without selection: regulated suppression of amber mutations in *Escherichia coli*. *Gene 311*, 153−163.
(50) Jordan, M., Schallhorn, A., and Wurm, F. M. (1996) Transfecting mammalian cells: optimization of critical parameters affecting calcium-phosphate precipitate formation. *Nucleic Acids Res. 24*, 596−601.